



Original Article

# Densification Mechanism and Structural Transformation in Glass: Molecular Dynamic Simulation

Nguyen Thi Thanh Ha\*

*School of Engineering Physics, Hanoi University of Science and Technology,  
1 Dai Co Viet, Hanoi, Vietnam*

Received 21 April 2024

Revised 6 June 2024; Accepted 29 July 2024

**Abstract:** The structure of  $\text{GeO}_2$  glass is investigated via molecular dynamic simulation. The influence of pressure to the structure of  $\text{GeO}_2$  glass is due to the change of short-range order, network structure, domain structure and free volume regions. The obtained results show that the structure of  $\text{GeO}_2$  was formed by a continuous random network of basic structural units linking to each other via with corner-sharing, edge-sharing, face-sharing bond. At low pressure, the basic structural units are mainly linked via one bridge oxygen (the corner sharing bonds). As pressure increases, the fraction of edge sharing bonds (two bridge oxygen) increases meanwhile the fraction of corner sharing bonds significantly decrease. There is a slight increase with the fraction of face-sharing bonds (three bridge oxygen). The Ge-O bond distance is almost not dependent on pressure, meanwhile the Ge-Ge and O-O bond distances are significantly dependent on pressure. Under compression, the average coordination number of Ge tends to increase from fourfold (at ambient pressure) to six-fold (at high pressure). Moreover, structure of  $\text{GeO}_2$  glass has two-domain near 15 and 25 GPa. And at ambient pressure or high pressures, the structure of  $\text{GeO}_2$  glass has single domain. The dependence of the distribution of free volumes on pressure in  $\text{GeO}_2$  glass has been examined. The distribution of void radius has the Gaussian form and the position of the peak tend to shift to the left under compression.

*Keyword:* Molecular dynamic, glass, domain structure, pressure, free volumes.

## 1. Introduction

In recent decades, numerous studies have focused on the structure and dynamical characteristic of oxide glasses. This is because they are important materials that have been widely applied in many fields

\* Corresponding author.

*E-mail address:* [ha.nguyenthithanh1@hust.edu.vn](mailto:ha.nguyenthithanh1@hust.edu.vn)

<https://doi.org/10.25073/2588-1124/vnumap.4927>

such as: microelectronics device, optical fiber, medicine (bio-material) and certain adsorption materials. It is known that the structure of oxide glasses like silica ( $\text{SiO}_2$ ), borate ( $\text{B}_2\text{O}_3$ ), germania ( $\text{GeO}_2$ ), alumina ( $\text{Al}_2\text{O}_3$ ) comprises basic structural units. Their structures are formed by a continuous random network of corner-shared tetrahedrons, in which a random structure is generated by linking short-range structural units with relatively narrow range of bond angle distribution [1-3]. The pressure influence of the structural transformation of oxide glasses has been investigated in detail. Upon compression at high pressure, there is a progressively structural transition from tetrahedral structure to octahedral structure and most of basic structural units transform to  $\text{TO}_4$  (T= Si, Ge, Al, B, ect.). At more elevated pressures, most of the basic structural units are  $\text{TO}_6$ , forming an octahedral network [4-8]. Furthermore, the T-O bond length and T-O coordination number increase with the increase of pressure. The Si-O distance is close to 1.62 Å. The distribution of the Si-O-Si bond angle has a maximum of  $144^\circ$  indicating the distinction between vitreous and crystalline forms of silica. The O-Si-O bond angle also gives a broad distribution with a maximum of  $109^\circ$  [9-10]. Under the change from low-density, the Al-O bond length increases from 1.74 to 1.80 Å. The Al-O-Al bond angle has a wide range of values from  $93^\circ$  to  $130.3^\circ$ . At high density, it has a peak at  $75^\circ$  but when the density decreases the peak shifts toward a larger value, namely  $107^\circ \pm 3^\circ$  [11, 12].

With  $\text{GeO}_2$ , the experimental studies show that at ambient pressure, the average distances for the Ge-Ge, Ge-O and O-O pairs are 3.16- 3.18, 1.73 and 2.83 Å, respectively. The average bond angles for the O-Ge-O and Ge-O-Ge are equal to  $109^\circ$  and  $133^\circ$  [7, 8, 11]. Under compression, the average Ge-O bond length increases from 1.72 Å (at ambient pressure) to 1.82 Å (at 13 GPa). The average bond angles for the O-Ge-O and Ge-O-Ge are significantly dependent on pressure. The O-Ge-O and Ge-O-Ge angles decrease with increasing pressure. Moreover, many researchers have revealed that  $\text{GeO}_2$  has a slightly distorted tetrahedral network structure like  $\text{SiO}_2$  [12, 13]. The aim of this work is to research the influence of pressure on the short-range order, network structure, domain structure and free volume regions of  $\text{GeO}_2$  glass at 600 K, then to clarify densification mechanism and structural transformation in oxide glasses.

## 2. Computational Procedure

Molecular dynamic simulations were performed for  $\text{GeO}_2$  system (5,400 atoms including 1,833 of Ge and 3,666 of O) at 600 K, under pressure ranging from 0 to 100 GPa. We used periodic boundary conditions and Oeffner-Elliott potentials [14, 15]. The Verlet algorithm time step of 0.5 fs is used to integrate the motion equation. To obtain the  $\text{GeO}_2$  model at 0 GPa, the initial configuration was constructed by randomly placing all atoms in a simulation box. This configuration was heated to 6,000 K to avoid the effects of the initial state on the system. Then the sample was cooled down to 3,500 K. The model has relaxed in the NPT (ensemble at this temperature for 4.0-5.0 ns). This is call model M1 (0 Gpa; 3,500 K). The  $\text{GeO}_2$  models (3, 6, 9, 12, 15, 20, 30, 40, 60, 80, 100 GPa) were constructed starting from the configuration with a pressure of 0 GPa. After that, the models are cooled to 600 K with cooling rate of 2.5 K/ps. These models are relaxed for  $10^6$  MD time. In order to improve statistics, all quantities of considered structural data were calculated by averaging over 10,000 configurations during the last simulation.

We use the cutoff distances  $r_{\text{cutoff}}$  (the first minimum of pair radial distribution function) to calculate the number of  $\text{GeO}_x$  unit.  $r_{\text{cutoff}}$  is equal to 2.54 Å for Ge-O pair. The schematic illustration of coordination number and domain D4 is shown in Fig. 1. There are two types of the bridge oxygen. The first type is bonded with Ge atoms having the same coordination numbers. In contrast, the second type is connected with Ge atoms having different coordination numbers. It is boundary oxygen (DB).  $D_x$

domain comprises O and Ge atoms having the same coordination numbers. Figure 1c presents domain D4 with 3 atoms: two  $\text{Ge}^4$  atoms and one  $\text{O}_{44}$  atom.

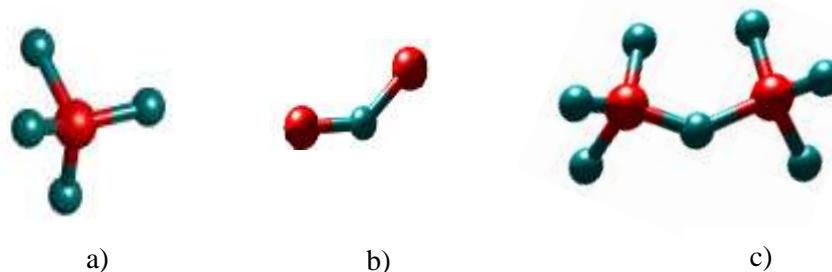


Figure 1. The schematic illustration of (a) and (b) the coordination number  $\text{GeO}_4$ ,  $\text{OGe}_2$ , (c) domain D4 with 3 atoms.

The structure of  $\text{GeO}_2$  is formed by a continuous random network of basic structural units linking to each other via with one (corner-sharing bond), two (edge-sharing bond) and three (face-sharing bond) bridging oxygens (BOs). Fig. 2 displays the  $\text{GeO}_x$ - cluster, consisting three types of sharing in structure of  $\text{GeO}_2$  glass.



Figure 2. Schematic illustration of  $\text{GeO}_x$ - cluster consist three type of sharing bonds.

### 3. Results and Discussion

To determine the influence of pressure on structural characteristics in  $\text{GeO}_2$  glass, we have constructed 12 configurations in the range of pressure from 0 to 100 GPa, 600 K. Firstly, the structural characteristics of  $\text{GeO}_2$  glass is compared to experimental data, and therefore allow us to test the reliability of models. The position and height of first peak in PRDF  $g_{ij}(r)$  and fraction of basic structural units of model and experiment are shown in Table 1. The obtained results show that the bond Ge-O bond distance is almost not dependent on pressure. Namely, at lower 12 GPa, the Ge-O bond length is around 1.74 Å. It has maximum value of approximately 1.80 Å at 30 GPa. And the Ge-O bond length almost does not change with pressure. It has value about 1.78 Å at pressure beyond 40 GPa. The result is in good agreement with values reported in [11, 16]. However, the Ge-Ge and O-O bond distances are significantly dependent on pressure. The Ge-Ge and O-O bond lengths are around 3.16 Å and 2.82 Å, respectively. The constructed models have the structural characteristics that are closed to the results in [17].

Moreover, the results shown in Table 1 revealed that the average coordination number of Ge tends to increase from four-fold (at ambient pressure) to six-fold (at high pressure). Namely, fraction of  $\text{GeO}_4$

monotonously decreases while fraction of GeO<sub>6</sub> increases with increasing pressure. The fraction of GeO<sub>5</sub> increases and has a maximum near the point of 15 GPa.

Table 1. Structural characteristics of GeO<sub>2</sub> glass;  $r_{ij}$  the position of first peak in *PRDF*;  $z_{ij}$  is the average coordination number

Model (GPa)	0	3	6	9	12	15	20	30	40	60	80	100	[11, 16]
$r_{Ge-Ge}$ , [Å]	3.16	3.16	3.20	3.26	3.36	3.34	3.20	3.40	3.36	3.34	3.34	3.30	3.16, 3.30
$r_{Ge-O}$ , [Å]	1.74	1.74	1.74	1.74	1.76	1.76	1.78	1.80	1.78	1.78	1.78	1.78	1.74 ± 0.02
$r_{O-O}$ , [Å]	2.82	2.80	2.76	2.70	2.66	2.64	2.62	2.60	2.58	2.54	2.54	2.50	2.80
$Z_{Ge-O}$	4.07	4.25	4.49	4.70	4.88	4.99	5.19	5.43	5.53	5.65	5.71	5.77	-
$Z_{O-Ge}$	1.99	2.08	2.19	2.29	2.34	2.39	2.43	2.47	2.51	2.52	2.49	2.49	-

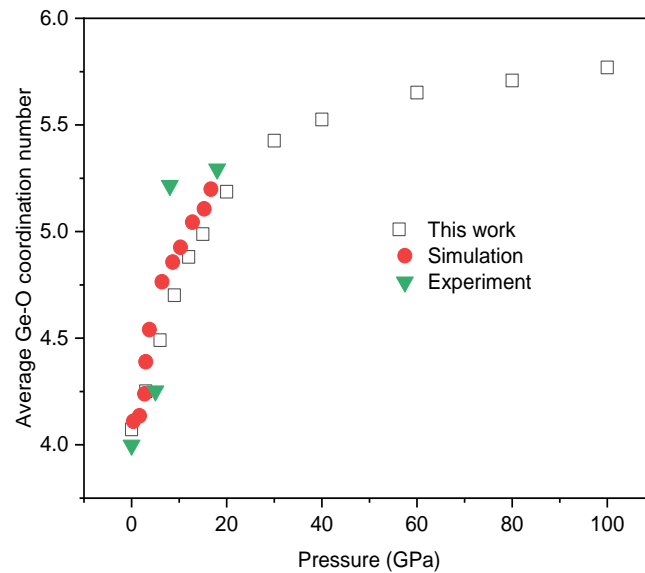


Figure 3. Pressure dependence of the average Ge-O coordination number (this study) compared to data from previous works: Simulation [18] and experiment [7].

Fig. 3 presents the average coordination number of Ge-O as a function of pressure. The results are compared to the data reported in previous works. There is an increase of the number of oxygen neighbors in the vicinity of a Ge atom. By inelastic X-ray scattering experiment, Lelong et al. showed that the coordination numbers increase to 5.3 under compression [7]. This result is observed via perform molecular dynamics simulation on amorphous GeO<sub>2</sub> under compression from 4.8 and 16.6 GPa [18].

The curve for the fraction of GeO<sub>5</sub> intersects with the one for the fraction of GeO<sub>4</sub> and the fraction of GeO<sub>6</sub> at 10 and 25 GPa, respectively (Fig. 4). Meanwhile, the average coordination number of oxygen tends to increase from two-fold (at ambient pressure) to three-fold (at high pressure) (Fig. 5).

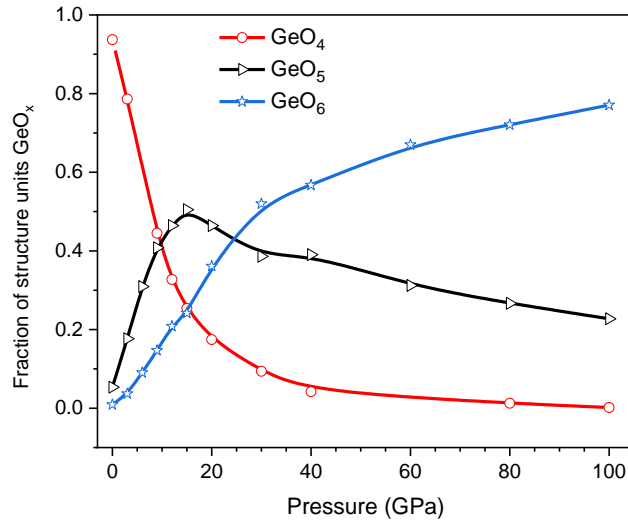


Figure 4. Pressure dependence of fraction of  $\text{GeO}_x$  units in  $\text{GeO}_2$  glass.

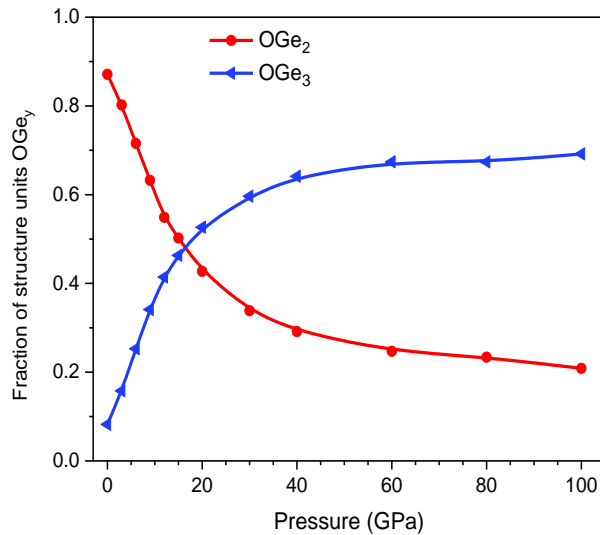


Figure 5. Pressure dependence of fraction of  $\text{OGe}_y$  units in  $\text{GeO}_2$  glass.

To clarify the structural transformation mechanisms, we consider the dependence on pressure of the  $\text{D}_x$  domain, distribution of Core-, Edge and Face- sharing bond and the distribution of free volumes in  $\text{GeO}_2$  glass. Fig. 6 shows the dependence of domain atoms on the pressure. The results reveal that there is two-domain ( $\text{D}_4$ - $\text{D}_5$  or  $\text{D}_5$ - $\text{D}_6$ ) near 15 and 25 GPa. And at ambient pressure or high pressure, structure of  $\text{GeO}_2$  glass has one domain ( $\text{D}_4$  or  $\text{D}_6$  domain) BD. The fraction of DB has maximum near the point of 15 GPa. The change of the fraction of DB can be explained as following, the merging of  $\text{D}_x$  domains intensively occurs at low or high pressures, meanwhile the splitting of domain intensively occurs around 15 GPa. The total of number of  $\text{D}_x$  domain has maximum value of 703 at 15 GPa. This result is presented in Table 2.

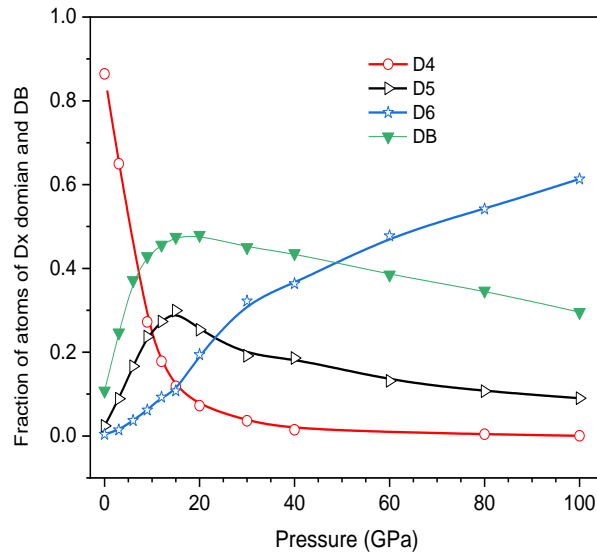


Figure 6. The dependence of domain atoms on the pressure in GeO<sub>2</sub> glass.

Table 2. The number of domains in GeO<sub>2</sub> glass. In which  $N_{D4}$ ,  $N_{D5}$ ,  $N_{D6}$  is the number of D4-, D5- and D6-domain, respectively

Model (GPa)	$N_{D4}$	$N_{D5}$	$N_{D6}$	Total number
0	1	66	14	81
3	11	156	55	222
6	74	206	125	405
9	156	185	190	531
12	223	168	231	622
15	274	169	260	703
20	144	297	117	558
30	240	242	195	677
40	73	342	67	482
60	33	381	26	440
80	22	362	20	404
100	3	319	8	330

One can see that, at low pressures, there is only one large D4 domain at ambient pressure. The large D4 domain is broken into small ones and it has a maximum value near a point of 15 GPa. At pressure beyond 30 GPa, the decreasing number of D4 domains is caused by decreasing number of GeO<sub>4</sub>. Under compression, there is a gradually structural transition from a tetrahedral structure (GeO<sub>4</sub> units) to an octahedral structure (GeO<sub>6</sub> units) via intermediated GeO<sub>5</sub> unit. Therefore, the number of GeO<sub>6</sub> increases and the number of D6 domain decreases. The small D6 domains has been merged into large ones. The number of D6 domain significantly decreases under compression. At high pressure (100 GPa) the number of D6 domain is equal to 3. Moreover, the intensive splitting of D5 domain and merging of D6 domains occurs parallel at pressures larger than 15 GPa. So, the number of boundary atom oxygen increases within 0 - 15 GPa and decreases at pressure beyond 30 GPa.

To clarify the dependence of the number of corner-, edge- and face-sharing bonds on compression, we calculated the distribution of the number of corner-, edge- and face-sharing bonds as well as their

length at different pressures. The obtained results are shown in Table 3 and 4. At low pressure, the basic structural units are mainly linked via bridge oxygen (BO) and the connectivity between  $\text{GeO}_x$  is mainly one BO (the corner sharing bonds). The fraction of corner sharing bonds is equal to 95.13% total of bond. The fraction of edge-, and face-sharing bonds is quite small (equal to 4.57% and 0.31%, respectively). At high pressure (100 GPa), the number of corner-, edge- and face-sharing bonds is 5,579; 1,814 and 443, (equal to 71.20%, 23.15% and 5.65%, respectively). As pressure increases, fraction of edge sharing bonds increases meanwhile fraction of corner sharing bonds significantly decreases. There is a slight increase with the fraction of face- sharing bonds.

Table 3. The distribution of Core-, Edge and Face- sharing bond at different pressures in  $\text{GeO}_2$  glass.  $N_{\text{core}}$ ,  $N_{\text{edge}}$ ,  $N_{\text{face}}$ ,  $C_{\text{core}}$ ,  $C_{\text{edge}}$  and  $C_{\text{face}}$  is the number and fraction of core-, edge and face- sharing bond, respectively

P(GPa)	$N_{\text{core}}$	$N_{\text{edge}}$	$N_{\text{face}}$	$C_{\text{core}}$ (%)	$C_{\text{edge}}$ (%)	$C_{\text{face}}$ (%)
0	3708	178	12	95.13	4.57	0.31
3	3830	389	42	89.89	9.13	0.99
6	3995	647	100	84.25	13.64	2.11
9	4162	863	156	80.33	16.66	3.01
12	4250	1114	187	76.56	20.07	3.37
15	4397	1178	229	75.76	20.30	3.95
20	4470	1486	260	71.91	23.91	4.18
30	4819	1573	407	70.88	23.14	5.99
40	4918	1748	382	69.78	24.80	5.42
60	5203	1797	421	70.11	24.22	5.67
80	5450	1773	442	71.10	23.13	5.77
100	5579	1814	443	71.20	23.15	5.65

Table 4. The distribution of average corner-, edge-, face-sharing bond length at different pressures in  $\text{GeO}_2$  glass.  $D_c$ ,  $D_e$  and  $D_f$  are the average-distance of corner-sharing bonds, edge-sharing bonds and face-sharing bonds, respectively

P(GPa)	$D_c$ (Å)	$D_e$ (Å)	$D_f$ (Å)
0	3.2044	2.5296	2.3773
3	3.2243	2.6193	2.3515
6	3.2627	2.6359	2.3653
9	3.2859	2.6657	2.3349
12	3.3148	2.6728	2.3474
15	3.3248	2.6715	2.3421
20	3.3556	2.6893	2.3507
30	3.3766	2.7020	2.3418
40	3.3771	2.6923	2.3494
60	3.3671	2.6858	2.3407
80	3.3468	2.6767	2.3326
100	3.3342	2.6660	2.3154

The pressure dependence of distribution of average corner-, edge-, face-sharing bond lengths is presented in Table 4. One can see that the average corner sharing bond lengths is about 3.204 Å at ambient pressure. In the 0–40 GPa pressure range, the average corner sharing bond lengths significantly increase with pressure and get maximum value of 3.377 Å at 40 GPa. At 100 GPa pressure, it is about

3.334 Å. Moreover, the result also shows the increase of the average edge-sharing bond lengths with compression. At 30 GPa, the average lengths of edge-sharing bonds were around 2.702 Å. However, the increase of the average edge-sharing bond lengths is small. Meanwhile the average length of face-sharing bonds is almost not dependent on pressure. In the 12–60 GPa pressure range, it is around 3.34-3.35 Å. In the 0–9 GPa pressure range, the number of face-sharing bonds is too small to calculate the average length.

In the structure of materials, there is an existence of free volume regions. So, we calculate the dependence of distribution of free volumes on pressure in GeO<sub>2</sub> glass, in which the void is a sphere passing four neighboring atoms without atom inside. The radius of the void is not fixed, it depends only on position of four atoms. The radius distribution of the void is given in Fig. 7. It can be seen that the distribution of the void radius has the Gaussian form. The position of the peak tends to shift to the left under compression. At 0–100 GPa range, the position of the peak of fraction of the void radius shifts from 1 Å to 0.75 Å.

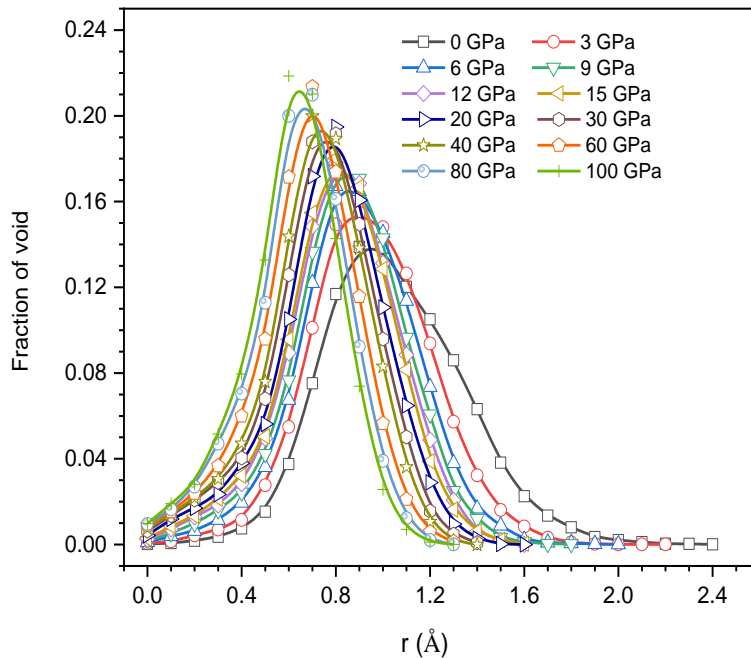


Figure 6. The radius distribution of void in GeO<sub>2</sub> glass under ompression.

The free volume characteristics in GeO<sub>2</sub> glass is described in Table 5, here we call the voids that have the radius greater than or equal to the oxygen atom are vacancies. Under compression, the number of void increases from 22,390 to 24,430 meanwhile the number of vacancies decreased from 1,811 at 0 GPa to 2 at 20 GPa. Because of a significant role of vacancies in the diffusion mechanism of the system, the diffusion process almost does not occur. The number of void clusters also increased linearly with the compression from 3,761 clusters at 0 GPa to 7,375 clusters at 100 GPa. Thus, at the high pressure there are many small clusters of voids. These results are closed to volume of cluster of voids. One can see that the volume of cluster of the voids strongly depends on the pressure. It reduces from 1.28 to 0.64 with increasing compression.



Table 5. Free volume characteristics in GeO<sub>2</sub> glass. In which,  $N_{void}$ ,  $N_{cav}$  and  $N_{cluster}$  are the number of voids, vacancies, and cluster of voids, respectively.  $V_{void}$  and  $V_{cl}$  is the volume of cluster of voids, respectively

Model (GPa)	$N_{void}$	$N_{cav}$	$N_{cluster}$	$V_{void}$	$V_{cl}$
0	22390	1811	3761	0.5114	1.28
3	23102	572	4444	0.4657	1.16
6	23322	237	4893	0.4338	1.10
9	23603	96	5263	0.4003	0.98
12	23577	35	5461	0.3939	0.90
15	23493	40	5643	0.3824	0.96
20	23349	2	5559	0.3608	0.78
30	22002	1	5901	0.3852	0.86
40	22817	2	5973	0.3794	0.75
60	23860	0	6581	0.3024	0.68
80	24276	0	7098	0.2843	0.61
100	24430	0	7375	0.2706	0.64

#### 4. Conclusion

The influence of pressure to the structure of GeO<sub>2</sub> glass is investigated via molecular dynamic simulation. The obtained results show that the structure of GeO<sub>2</sub> is formed by a continuous random network of basic structural units linking to each other via with corner-sharing, edge-sharing, face-sharing bond.

The bond Ge-O bond distance is almost not dependent on pressure meanwhile the Ge-Ge and O-O bond distance is significantly dependent on pressure. At ambient pressure, the Ge-O bond length is around 1.74 Å; the Ge-Ge and O-O bond length is around 3.16 Å and 2.82 Å, respectively. And the basic structural units are mainly linked via the corner sharing bonds. The average corner sharing bond lengths is about 3.204 Å at 0 GPa. As pressure increases, fraction of edge sharing bonds and fraction of face-sharing bonds increase meanwhile fraction of corner sharing bonds significantly decrease.

The average length of face-sharing bonds is almost not dependent on pressure. It is around 3.34-3.35 Å. Moreover, the distribution of free volumes depends on pressure. The distribution of void radius has the Gaussian form and the position of the peak tends to shift to the left under compression. As pressure increases, the void radius decreases rapidly.

#### Reference

- [1] M. C. Wilding, M. Wilson, P. F. McMillan, Structural Studies and Polymorphism in Amorphous Solids and Liquids at High Pressure, Chem. Soc. Rev, Vol. 35, No. 10, 2006, pp. 964-986, <https://doi.org/10.1039/B517775H>.
- [2] J. Peralta, G. Gutierrez, Pressure-induced Structural Transition in Amorphous GeO<sub>2</sub>: a Molecular Dynamics Simulation, Eur. Phys. J. B, Vol. 87, No. 11, 2014, pp. 257-266, <https://doi.org/10.1140/epjb/e2014-50176-3>.
- [3] B. Walker, C. C. Dharmawardhana, N. Dari, P. I. Rulis, W. Ching, Electronic Structure and Optical Properties of Amorphous GeO<sub>2</sub> Incomparison to Amorphous SiO<sub>2</sub>, J. Non-Cryst, Solids, Vol. 428, 2015, pp. 176-183, <https://doi.org/10.1016/j.jnoncrsol.2015.08.018>.

- [4] J. F. Lin, H. Fukui, D. Prendergast, T. Okuchi, Y. Q. Cai, N. Hiraoka, C. S. Yoo, A. Trave, P. Eng, M. Y. Hu, P. Chow, Electronic Bonding Transition in Compressed SiO<sub>2</sub> Glass, *Phys. Rev. B*, Vol. 75, No. 1, 2007, pp. 012201-012205, <https://doi.org/10.1103/PhysRevB.75.012201>.
- [5] Y. Liang, C. R. Miranda, S. Scandolo, Tuning Oxygen Packing in Silica by Nonhydrostatic Pressure, *Phys. Rev. B*, Vol. 99, No. 21, 2007, pp. 215504-215509, <https://doi.org/10.1103/PhysRevLett.99.215504>.
- [6] L. Huang, J. Kieffer, Amorphous-Amorphous Transitions in Silica Glass, I Reversible Transitions and Thermo-Mechanical Anomalies, *Phys. Rev. B*, Vol. 69, No. 22, 2004, pp. 224203-224214, <https://doi.org/10.1103/PhysRevB.69.224203>.
- [7] G. Lelong, L. Cormier, G. Ferlat, V. Giordano, G.S. Henderson, A. Shukla and G. Calas, Evidence of fivefold-coordinated Ge atoms in amorphous GeO<sub>2</sub> under pressure using inelastic x-ray scattering, *Phys. Rev. B*, Vol. 85, No.13, 2012, pp. 134202-134207. <https://doi.org/10.1103/PhysRevB.85.134202>.
- [8] Y. Lin, Q. Zeng, W. Yang, W. L. Mao, Pressure-induced Densification in GeO<sub>2</sub> Glass: A Transmission X-Ray Microscopy Study, *Appl. Phys. Lett*, Vol. 103, No. 26, 2013, pp. 261909-261914, <https://doi.org/10.1063/1.4860993>.
- [9] Q. Mei, C. J. Benmore, J. K. R. Weber, Structure of Liquid SiO<sub>2</sub>: A Measurement by High-Energy X-Ray Diffraction, *Phys. Rev. Lett*, Vol. 98, No. 5, 2007, pp. 057802-057806, <https://doi.org/10.1103/PhysRevLett.98.057802>.
- [10] V. V. Le , G. T. Nguyen, Molecular Dynamics Study of Mechanical Behavior in Silica Glass Under Uniaxial Deformation, *Computational Materials Science*, Vol. 159, 2019, pp. 385-396, <https://doi.org/10.1016/j.commatsci.2018.12.045>.
- [11] X. Hong, M. Newville, T. S. Duffy, S. R. Sutton, M. L. Rivers, X-ray Absorption Spectroscopy of GeO<sub>2</sub> Glass to 64 GPa, *J. Phys., Condens. Matter*, Vol. 26, No. 3, 2014, pp. 03510-03519, <https://doi.org/10.1088/0953-8984/26/3/035104>.
- [12] V. V. Hoang, Static and Dynamic Properties of Simulated Liquid and Amorphous GeO<sub>2</sub>, *J. Phys.: Condens. Matter*, Vol. 18, No. 3, 2005, pp. 777-786, <https://doi.org/10.1088/0953-8984/18/3/003>.
- [13] V. V. Hoang, N. H. T. Anh, H. Zung, Liquid-liquid Phase Transition and Anomalous Diffusion in Simulated Liquid GeO<sub>2</sub>, *Phys. B: Condens. Matter*, Vol. 390, No. 1-2, 2007, pp 17-22, <https://doi.org/10.1016/j.physb.2006.07.021>.
- [14] D. Marrocchelli, M. Salanne, P. A. Madden, C. Simon, P. Turq, The Construction of a Reliable Potential for GeO<sub>2</sub> from First Principles, *Mol.Phys*, Vol. 107, No. 4-6, 2009, pp. 443-452, <https://doi.org/10.1080/00268970902845347>.
- [15] D. Marrocchelli, M. Salanne, P. A. Madden, High-pressure Behaviour of GeO<sub>2</sub>: A Simulation Study, *J. Phys. Condens. Matter*, Vol. 22, No. 15, 2010, pp. 443-452, <https://doi.org/10.1088/0953-8984/22/15/152102>.
- [16] J. W. E. Drewitt, P. S. Salmon, A. C. Barnes, S. Klotz, H. E. Fischer, W. A. Crichto, Structure of GeO<sub>2</sub> Glass at Pressures up to 8.6 GPa, *Phys. Rev. B*, Vol. 81, No. 1, 2010, pp. 014202-014215, <https://doi.org/10.1103/PhysRevB.81.014202>.
- [17] X. Hong, L. Ehm, T. S. Duffy, Polyhedral Units and Network Connectivity in GeO<sub>2</sub> Glass at High Pressure: an X-Ray Total Scattering Investigation *Appl. Phys. Lett*, Vol. 105, No. 8, 2014, pp. 081904-081909, <https://doi.org/10.1063/1.4894103>.
- [18] M. Micoulaut, Structure of Densified Amorphous Germanium Dioxide, *J. Phys.: Condens. Matter*, Vol. 16, No. 10, 2004, pp. L131- L138, <https://doi.org/10.1088/0953-8984/16/10/L03>.